Theoretical Analysis of Resonant Frequency for AMC-based Absorber Composed of Square Patch Array

Levy Olivia Nur[1,2], Adit Kurniawan[1], Sugihartono[1], and Achmad Munir[1]

[1]Radio Telecommunication and Microwave Laboratory
School of Electrical Engineering and Informatics, Institut Teknologi Bandung
Jalan Ganesha 10, Bandung 40132, Indonesia
[2]School of Electrical Engineering, Telkom University
Jalan Telekomunikasi, Dayeuh Kolot, Bandung 40257, Indonesia
munir@ieee.org

Abstract: The new formulation of resonant frequency for absorber based on artificial magnetic conductor (AMC) structure composed of square patch array is investigated theoretically based on analytical approach. The investigation is performed to define the resonant frequency using equivalent LC circuit model from the physical dimension and material property of square patch array. The proposed equivalent LC circuit model formulas are derived using the conformal mapping theory for the adjacent co-planar square patches and the Gauss' law and Faraday's law for the square patch parallel with the ground plane. The analytical approach is then examined and compared with the numerical results of AMC structure simulated by use of commercialized software. Here, the AMC structure consists of a two-dimensionally (2D) array square patches deployed on a dielectric substrate. The frequency range of analysis which is observed from 1-5 GHz corresponds to the working frequency of square patch. Hence, the analyzed parameters of square patch, i.e. unit cell, include substrate width, substrate thickness, substrate properties, patch width, and the gap between patches. It shows that the proposed formulation of equivalent LC circuit model yields better results compared to the existing formulation. Moreover, the proposed formulation shows the bandpass-like structure in which the waves are absorbed in a certain value of frequency band. This is appropriate to the absorbance concept where some absorber will restrain the energy from incoming waves.

Keywords: Absorber, artificial magnetic conductor, square patch, resonant frequency.

1. Introduction

In recent times, the electromagnetic metamaterials, in other term known as artificial materials, have attracted a lot of attention due to their unique properties for various electromagnetic purposes [1]-[3]. In many cases, the use of electrical conductors can affect the performance of electromagnetic devices particularly those that involve radio communications. Moreover, the requirements of high performance conductive surface become higher as the wide applications of the surface in electromagnetic devices. One technique that has been attracted many researchers to improve the electromagnetic properties is modifications the textures of a metal surface [4]-[7]. Currently, the use of texture modifications yielded more variety of applications including the wave guide, antennas, radar, left handed media and any others. The unique properties including having better performance in controlling the propagation of electromagnetic waves make the materials able to solve the problem of antennas and microwave devices [8]-[9].

These high functionality artificial materials include all kind of materials which have unique properties that are different from ordinary materials. One of the artificial materials, namely artificial magnetic conductor (AMC) recently has attracted researchers and

Received: February 14th, 2015. Accepted: June 18th, 2015
DOI: 10.15676/ijeei.2015.7.2.9

practitioners in electromagnetic community to involve it in the design of highly efficient and low-profile antennas [4]-[5], [8]-[9]. Basically, the AMC has a physical approximation of the perfect magnetic conductor (PMC). Since in reality the PMC is very difficult to be implemented, thus a medium which is capable to approach PMC properties is very interesting to be explored. Furthermore, AMCs are PMCs material-like and are dual to a perfect electric conductor (PEC) from an electromagnetic point of view.

In this paper, a novel approach to formulate the resonant frequency of absorber based on AMC structure composed of square patch array is investigated. The goal of the approach is to obtain one of most important properties of the structure which is proposed as PMC material-like. By obtaining the formulation of resonant frequency, the parameter of AMC structure composed of square patch array can be exactly determined according to the design requirements. The investigation is performed based on the physical dimension and material property of square patch array used as AMC structure. The approach which is implemented by use of equivalent LC circuit model is addressed to be a complement of existing formulation in [10] which ignores some critical parameters in the calculation. To verify the approach, the proposed formulation is then examined through simulation of commercialized software and analyzed using regression methods. Some numerical results of proposed formulation in comparison to the simulation results and existing formulation are presented to demonstrate the capability and accuracy of the approach.

2. Theoretical Formulation and Equivalent Circuit Model

Basically, the AMC can be designed by configuring periodically patches in some array. The AMC has the high impedance electromagnetic structure surface which has been investigated by preparing metal plates periodically and connecting them to the groundplane trough conducting vias [4]-[5], [8]. In practice, the difficult process in fabrications of periodic metal plat forces the researcher to design in a planar configuration without via connection [6]-[7]. The structure of AMC is constructed of a square patch array in periodic arrangement and connected to the groundplane by the dielectric system instead of via. Figure 1 shows the illustration of AMC structure consists of a 2D array of unit cells in which each unit cell is built from a square patch placed on a grounded dielectric substrate.

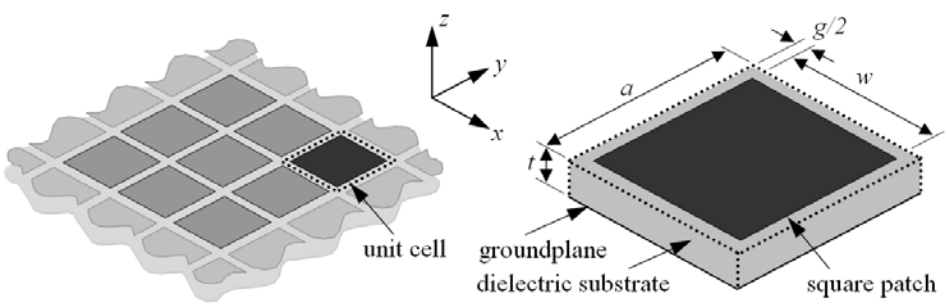

Figure 1. AMC structure consists of a 2D array of unit cells of square patch

In the design of AMC-based absorber, working frequency of the absorber is a first property that should be determined. Here, the working frequency of absorber depends on the structure of AMC which is constructed of a square patch array on a grounded dielectric substrate, namely unit cell. Hence, the AMC structure will work based on the resonant frequency of its unit cell. For the AMC structure shown in Figure 1, the resonant frequency can be obtained theoretically from the dimension and property of a unit cell by taking into account the size of patch, the gap between patch, the size of unit cell, the thickness of dielectric substrate, and the relative permittivity and permeability of dielectric substrate. The dimension and property of a unit cell

will produce the capacitance and inductance where both parameters will be useful for analyzing the AMC structure using the theory of circuit.

By employing a conformal transformation method to assist calculations of two-dimensionally electrostatic field distribution [11], the value of capacitance and inductance between the adjacent patches is derived. In later, the capacitance and inductance of adjacent co-planar square patches are referred as series capacitance and series inductance, respectively. At first, the method is applied for the calculation of large amount of capacitance in the adjacent co-planar square patches. In the calculation, a complex variable theory is used as expressed in (1)-(2).

$$\boldsymbol{r} = \sqrt{\boldsymbol{x}^2 + \boldsymbol{y}^2}\ ,\quad \theta = \mathbf{tan}^{-1}\left(\frac{\boldsymbol{y}}{\boldsymbol{x}}\right) \tag{1}$$

$$\boldsymbol{Z} = \boldsymbol{x} + \boldsymbol{jy} = \boldsymbol{r}\left(\mathbf{cos}\,\theta + \boldsymbol{j}\,\mathbf{sin}\,\theta\right) = \boldsymbol{re}^{\boldsymbol{j}\theta} \tag{2}$$

If another complex variable, for example W, exists and is given by (3),

$$\boldsymbol{W} = \boldsymbol{u} + \boldsymbol{jv} = \rho\boldsymbol{e}^{\boldsymbol{j}\varphi} \tag{3}$$

where W is a function of Z, every point of Z has a connection one-by-one with the value of W. The function of connection can be written in (4).

$$\boldsymbol{W} = \boldsymbol{f}\left(\boldsymbol{Z}\right) \tag{4}$$

If there is a change of ΔZ on the Z plane, for instance, it is coincidence with the change of ΔW on the W plane, the change of those values can be defined as a limit of the $\Delta W/\Delta Z$ as expressed in (5).

$$\frac{\boldsymbol{dW}}{\boldsymbol{dZ}} = \mathbf{lim}_{\Delta \boldsymbol{Z} \to 0}\frac{\Delta \boldsymbol{W}}{\Delta \boldsymbol{Z}} = \mathbf{lim}_{\Delta \boldsymbol{Z} \to 0}\frac{\boldsymbol{f}\left(\boldsymbol{Z} + \Delta \boldsymbol{Z}\right) - \boldsymbol{f}\left(\boldsymbol{Z}\right)}{\Delta \boldsymbol{Z}} \tag{5}$$

The complex function can be an analytic or a regular if the differential value is a unique. When the function is independent to a certain vector, the same result will be found if the value of Z is changed in x or y direction. Therefore, when the ΔZ equals Δx, (5) can be rewritten as given in (6).

$$\frac{\boldsymbol{dW}}{\boldsymbol{dZ}} = \frac{\partial \boldsymbol{W}}{\partial \boldsymbol{x}} = \frac{\partial}{\partial \boldsymbol{x}}\left(\boldsymbol{u} + \boldsymbol{jv}\right) = \frac{\partial \boldsymbol{u}}{\partial \boldsymbol{x}} + \boldsymbol{j}\frac{\partial \boldsymbol{v}}{\partial \boldsymbol{x}} \tag{6}$$

For the change of value in y direction, ΔZ equals Δy, it yields (7).

$$\frac{\boldsymbol{dW}}{\boldsymbol{dZ}} = \frac{\partial \boldsymbol{W}}{\partial\left(\boldsymbol{jy}\right)} = \frac{1}{\boldsymbol{j}}\frac{\partial}{\partial \boldsymbol{y}}\left(\boldsymbol{u} + \boldsymbol{jv}\right) = \frac{1}{\boldsymbol{j}}\frac{\partial \boldsymbol{u}}{\partial \boldsymbol{y}} + \frac{\partial \boldsymbol{v}}{\partial \boldsymbol{y}} = \frac{\partial \boldsymbol{v}}{\partial \boldsymbol{y}} - \boldsymbol{j}\frac{\partial \boldsymbol{u}}{\partial \boldsymbol{y}} \tag{7}$$

The two complex values will be same if and only if the real and imaginer value are the same. From (6) and (7), they will yield (8).

$$\frac{\partial \boldsymbol{u}}{\partial \boldsymbol{x}} = \frac{\partial \boldsymbol{v}}{\partial \boldsymbol{y}}\ ,\quad \frac{\partial \boldsymbol{v}}{\partial \boldsymbol{x}} = -\frac{\partial \boldsymbol{u}}{\partial \boldsymbol{y}} \tag{8}$$

The expression in (8) is known as Cauchy-Riemann equations. If it is assumed that u is an electric potential in volt, so the electric field (E) can be obtained from u and is a negative gradient of u, which is given in (9).

$$\boldsymbol{E_x = -\frac{\partial u}{\partial x}}, \quad \boldsymbol{E_y = -\frac{\partial u}{\partial y}} \tag{9}$$

To find the differential equation, the change on v would be coincided with the change on the x and y direction. Then, according to Cauchy-Riemann equations, the change on v can be expressed in term of electric field (E) or electric flux density (D) as given in (10) and (11), respectively.

$$\boldsymbol{-dv = \frac{\partial u}{\partial y}dx - \frac{\partial u}{\partial x}dy = -E_y dx + E_x dy} \tag{10}$$

$$\boldsymbol{-\varepsilon dv = -\varepsilon E_y dx + \varepsilon E_x dy = -D_y dx + D_x dy} \tag{11}$$

It is seen that the electric flux (ψ) changes proportionally to the change of electric flux density (D), therefore (11) can be expressed in (12) or (13).

$$\boldsymbol{-d\psi = \varepsilon dv} \tag{12}$$

$$\boldsymbol{-\psi = \varepsilon v} \tag{13}$$

To calculate the amount of electric flux on the adjacent co-planar square patches, the hyperbolic and elliptic conducting boundary would be used. The relations between W and Z are according to (14)-(17).

$$\boldsymbol{W = \cos^{-1} Z} \tag{14}$$

$$\boldsymbol{x + jy = \cos(u + jv) = \cos u \cosh v - j \sin u \sinh v} \tag{15}$$

$$\boldsymbol{x = \cos u \cosh v} \tag{16}$$

$$\boldsymbol{y = -\sin u \sinh v} \tag{17}$$

From (16) and (17), the hyperbolic function for x and y is given in (18)-(19).

$$\boldsymbol{\frac{x^2}{\cosh^2 v} + \frac{y^2}{\sinh^2 v} = 1} \tag{18}$$

$$\boldsymbol{\frac{x^2}{\cos^2 u} + \frac{y^2}{\sin^2 u} = 1} \tag{19}$$

For constant value of v, (18) represents a set of confocal ellipses with the foci at ±1, while for constant value of u (19) represents a set of confocal hyperbolas which are orthogonal to ellipses. Both hyperbolic functions are plotted in Figure 2. With a proper choice to serve as the potential function, the requirement of transformation can be solved.

Based on Figure 4, the field between infinite conducting patch and a perpendicular semi-infinite patch separated by a gap can be determined. The infinite patch is taken at a zero potential, while the perpendicular semi-infinite plane is taken at potential of V_0. The new scale factors should be put in using the results of the foregoing general transformations. Moreover, to

avoid the confusion with the preceding, the variables for the specific problem should be denoted by primes as given in (20).

$$\boldsymbol{W'} = \boldsymbol{C}_1 \cos^{-1} \boldsymbol{kZ'} + \boldsymbol{C}_2 \tag{20}$$

where the constant C_1 and C_2 are inserted to yield the proper scale of potential and to fix the reference for the potential, respectively, while the constant k to fix the size of patches. By comparing (20) with (14), a new expression is given in (21) yields to (22).

$$\boldsymbol{Z} = \boldsymbol{kZ'} \tag{21}$$

$$\boldsymbol{W'} = \boldsymbol{C}_1 \boldsymbol{W} + \boldsymbol{C}_2 \tag{22}$$

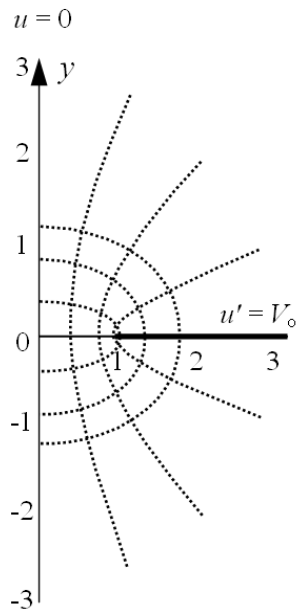

Figure 2. Hyperbolic function for field transformation

The constant C_1 and C_2 may be taken as real value for current problem, hence (22) can be rewritten in (23).

$$\boldsymbol{u'} = \boldsymbol{C}_1 \boldsymbol{u} + \boldsymbol{C}_2 \tag{23}$$

From Figure 2, it is seen that when u = 0 then $u'=V_o$ and when $u = \pi/2$ then u' = 0, therefore when $k = 1/p$ which produces $Z = Z'/p$, (20) can be rewritten in (24).

$$\boldsymbol{W'} = \boldsymbol{V_o}\left[1 - \frac{2}{\pi}\cos^{-1}\left(\frac{\boldsymbol{Z'}}{\boldsymbol{p}}\right)\right] \tag{24}$$

By applying trigonometrically function and substituting $\boldsymbol{W'} = \boldsymbol{u'} + \boldsymbol{jv'}$ in which $u' = V_o$, (24) can be given in (25).

$$\boldsymbol{v'} = -\frac{2\boldsymbol{V_o}}{\pi}\mathbf{cosh}^{-1}\left(\frac{\boldsymbol{Z'}}{\boldsymbol{p}}\right) \tag{25}$$

Then, by substituting (13) into (25), the electric flux across the patch can be obtained as expressed in (26).

$$\psi = \frac{2\varepsilon\boldsymbol{V_o}}{\pi}\mathbf{cosh}^{-1}\left(\frac{\boldsymbol{Z'}}{\boldsymbol{p}}\right) \tag{26}$$

If $Z' = a/2$ and $p = g/2$ for adjacent co-planar square patches shown in Figure 3, (26) can be rewritten in (27).

$$\psi = \frac{2\varepsilon\boldsymbol{V}}{\pi}\mathbf{cosh}^{-1}\left(\frac{\boldsymbol{a}}{\boldsymbol{g}}\right) \tag{27}$$

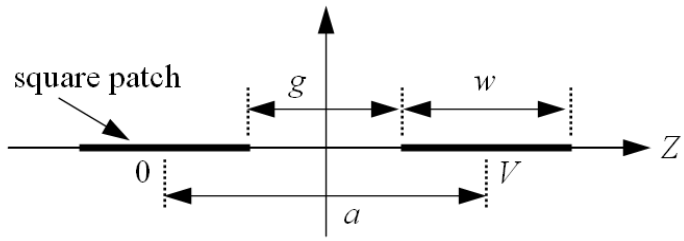

Figure 3. Structure of adjacent co-planar square patches

The electric flux at the end of patch equals to the charge on that patches. Hence, by using the relationship of flux and voltage, the capacitance per unit length for the structure can be obtained. In case the width of square patch is w as shown in Figure 3, the series capacitance of adjacent co-planar square patches in Farad (C_{sr}) can be expressed in (28).

$$\boldsymbol{C_{sr}} = \frac{2\varepsilon}{\pi\boldsymbol{w}}\mathbf{cosh}^{-1}\left(\frac{\boldsymbol{a}}{\boldsymbol{g}}\right) \tag{28}$$

By applying the same procedure, the series inductance of adjacent co-planar square patches in Henry which was ignored in [10] can be obtained as given in (29). It is noted all parameters related to electric field in obtaining the series capacitance value should be replaced with parameters of magnetic field such as permeability, magnetic potential, magnetic flux and magnetic flux density.

$$\boldsymbol{L_{sr}} = \frac{\pi\boldsymbol{w}\mu}{2\mathbf{cosh}^{-1}\left(\frac{\boldsymbol{a}}{\boldsymbol{g}}\right)} \tag{29}$$

Furthermore, the shunt capacitance between square path and ground plane can be derived by applying the Gauss' law for the electric flux density [12]. By assuming that the dielectric substrate is homogeneous and isotropic, as illustrated in Figure 1, for the dielectric substrate thickness (t) much smaller than the patch width, and the surface charge density at the surface is ρ_S, then the electric potential between square patch and ground plane can be written in (30).

$$\boldsymbol{v} = \frac{\boldsymbol{D}}{\varepsilon} \cdot \boldsymbol{t} = \frac{\rho_S \boldsymbol{t}}{\varepsilon} \tag{30}$$

Again, by using the relationship of flux and voltage, the capacitance per unit length between square patch and ground plane can be obtained. In case the width of square patch is w as shown in Figure 1, the capacitance between square patch and ground plane in Farad, later called as shunt capacitance (C_{sh}) which was ignored in [10], can be expressed in (31).

$$\boldsymbol{C_{sh}} = \frac{\varepsilon \boldsymbol{w}^2}{\boldsymbol{t}} \tag{31}$$

To obtain the shunt inductance, the same procedure can be applied by replacing Gauss' law with Faraday's law and all parameters related to electric field with parameters of magnetic field [12]. Hence, the value of inductance between square patch and ground plane (L_{sh}) is expressed in (32).

$$\boldsymbol{L_{sh}} = \mu \boldsymbol{t} \tag{32}$$

From the derivation of series capacitance and inductance as well as shunt capacitance and inductance, the equivalent circuit model of each unit cell of AMC structure is proposed as illustrated in Figure 4. It shows that C_{sr} and L_{sr} denote series capacitance and series inductance of square patch in a unit cell with the adjacent square patch, respectively, whilst C_{sh} and L_{sh} are shunt capacitance and shunt inductance between square patch and groundplane, respectively. The configuration of equivalent LC circuit behaves as 2D planar bandpass filters (BPF) which will work depend on the direction of incoming wave. The impedance of configuration plays an important thing in determining the resonant frequency of BPF and the level of absorbed incoming wave. Here, the impedance of configuration can be formulated from the series components, i.e. C_{sr} and L_{sr}, and shunt components, i.e. C_{sh} and L_{sh}.

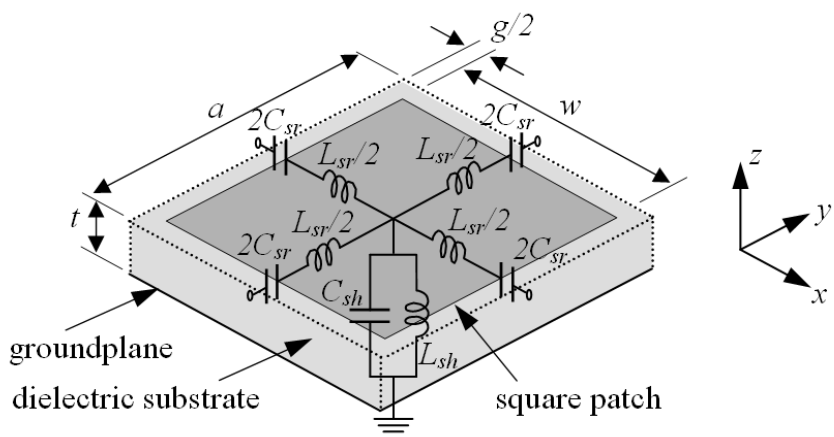

Figure 4. Equivalent circuit model of each unit cell of AMC structure

The resonant frequency of each BPF (f_0), for instance in x direction, can be derived by taking the real impedance part of configuration when the imaginary part is zero and is expressed in (33). It should be noted that by including the critical parameters, i.e. series inductance of adjacent co-planar square patches (L_{sr}) and shunt capacitance between square

patch and groundplane (C_{sh}), the formulation of resonant frequency becomes more general and will have more accurateness compared to the formulation in [10].

$$f_0 = \frac{1}{2\pi}\sqrt{\frac{\left(L_{sr}C_{sr} + L_{sh}C_{sh} + L_{sr}C_{sh}\right) + \sqrt{\left(L_{sr}C_{sr} + L_{sh}C_{sh} + L_{sr}C_{sh}\right)^2 - 4L_{sr}L_{sh}C_{sr}C_{sh}}}{2L_{sr}L_{sh}C_{sr}C_{sh}}} \tag{33}$$

3. Numerical Characterization and Result

Figure 5 illustrates a model to characterize the resonant frequency of a unit cell of AMC structure using commercialized simulation software. The unit cell arrangement constructed of a square patch on a grounded dielectric substrate is truncated by defining the perfect electric conductor (PEC) and the perfect magnetic conductor (PMC) boundary conditions on the sides that are perpendicular and parallel to the electric field (E) of incoming wave, respectively. Here, the boundary conditions are imaging the unit cell to form a double periodic array of infinite extent. It shows that the square patch has the width of w, periodicity or unit cell width of a, gap between patches of g, and dielectric substrate thickness of t. To obtain high accuracy simulation result which is implementable for experimental characterization, the thickness of square patch as well as groundplane which are made of metal copper is set to be 0.035mm. Moreover, the losses of dielectric substrate and metal copper are also taken into account.

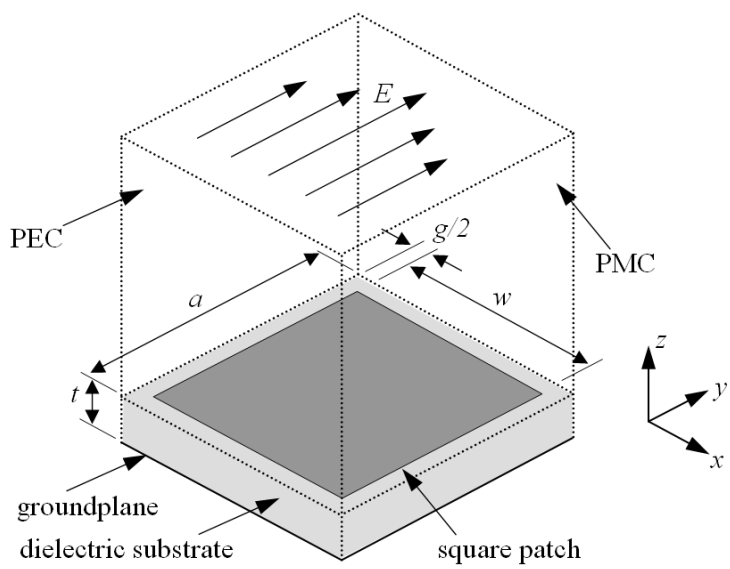

Figure 5. A model for characterizing resonant frequency of a unit cell of AMC structure

The characterization was carried out by varying the parameter of square patch and dielectric substrate including a, w, g, and t. There are five scenarios to characterize the resonant frequency of a unit cell of AMC structure by changing its physical dimension; (i) change the periodicity of substrate width (a) and the patch width (w) while keeping the gap between patches (g) to be constant; (ii) change the patch width (w) and the gap between patches (g) while keeping the periodicity (a) to be constant; (iii) change the periodicity (a) and patch width (w) while keeping the gap between patches (g) to be constant; (iv) change the patch width (w) while keeping the ratio of periodicity (a) and gap between patches (g) to be constant; (v) change the substrate thickness (t) while keeping other dimensions to be constant. The characterization result for each scenario in term of resonant frequency is plotted in Figures 6 – 10 with the proposed formulation result derived above and the existing formulation result form [10] depicted together in each variation of corresponding parameter for comparison.

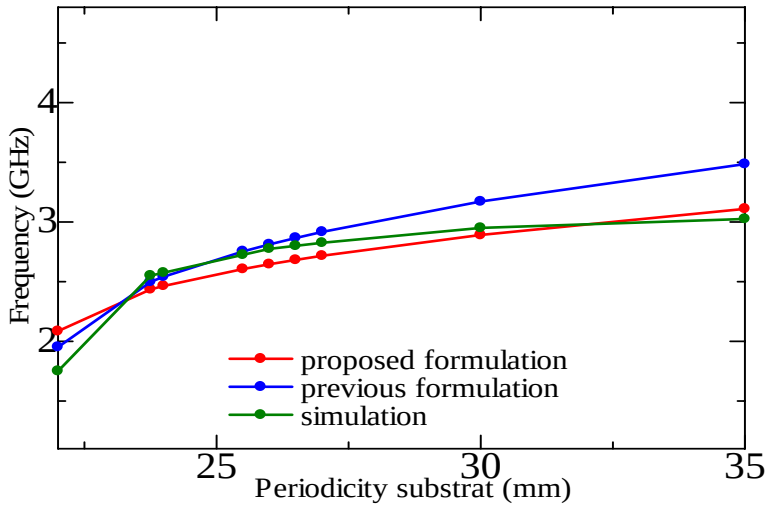

Figure 6. Comparison of resonant frequency for a unit cell with variation of periodicity (*a*) and gap between patches (*g*) while keeping patch width (*w*) to be constant

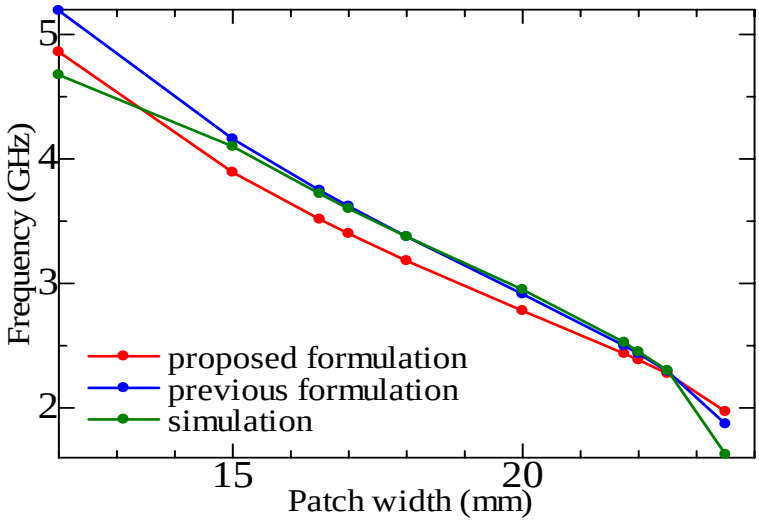

Figure 7. Comparison of resonant frequency for a unit cell with variation of patch width (*w*) and gap between patches (*g*) while keeping periodicity (*a*) to be constant

Figure 6 illustrates how the resonant frequency changes due to the variation of periodicity and gap between patches, and the remains of patch width. It shows when there is an enlargement of both periodicity (*a*) and gap between patches (*g*) while patch width (*w*) remains; it causes more dielectric layer areas which are not covered by square patch. Thus, it affects on its energy absorption which is greater for larger periodicity or gap between patches. From the fact, it shows that the value of proposed formulation, for periodicity of 30mm and above, is better than the previous formulation. The discrepancy between the simulation result and proposed formulation result in less than 2%.

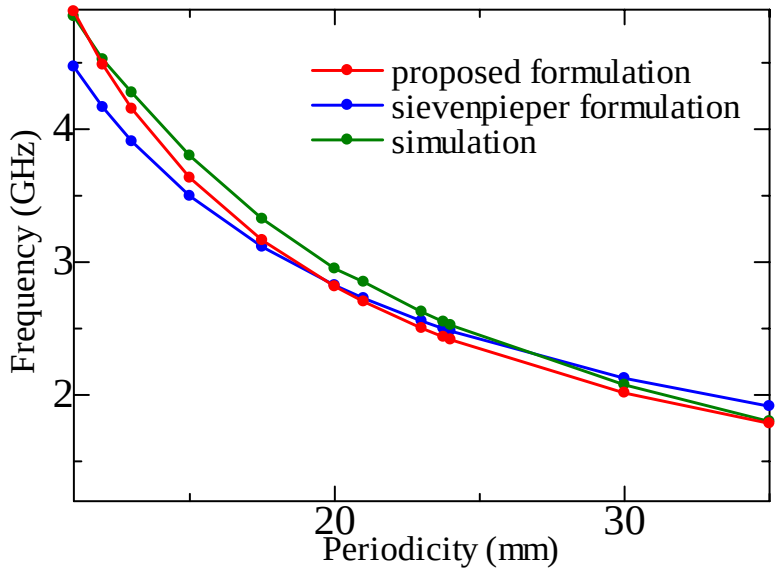

Figure 8. Comparison of resonant frequency for a unit cell with variation of periodicity (*a*) and patch width (*w*) while keeping gap between patches (*g*) to be constant

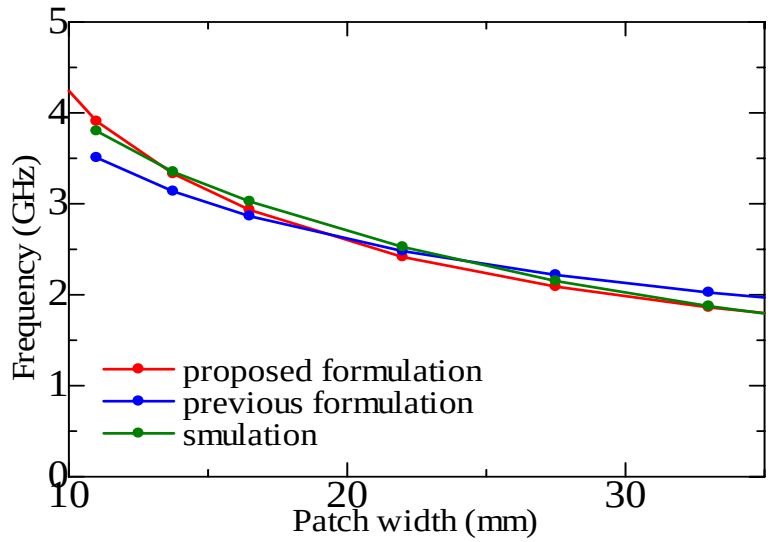

Figure 9. Comparison of resonant frequency for a unit cell with variation of patch width (*w*) while keeping the ratio of periodicity (*a*) and gap between patches (*g*) to be constant

Meanwhile, Figure 7 shows how the resonant frequency changes due to the variation of patch width and gap between patches and the remains of periodicity. When there is a variation of both gap between patches (*g*) and the patch width (*w*), while the periodicity (*a*) remains then it causes more dielectric layer areas which are covered by square patch. This is in contrast to the result in Figure 8. Therefore, it affects on its energy absorption which is lesser for wider patch width. From the result, it shows that the value of proposed formulation generates similar result to the simulation result for the patch width less 15mm.

In Figure 8, the resonant frequency of a unit cell of AMC structure which changes due to the variation of patch width and periodicity while keeping the gap between patches to be

constant is plotted. The graph shows that the size of patches is proportional to the size of substrate. Larger size of substrate utilizes larger size of patches. The trend in the change of resonant frequency is quite closed to the result in Figure 7. It shows that the value of proposed formulation produces quite similar result to the simulation result for the periodicity less than 17.5mm and greater than 30mm.

The comparison of resonant frequency for a unit cell of AMC structure with the variation of patch width and keeping the ratio of periodicity and gap between patches to be constant is depicted in Figure 9. The proposed formulation produces quite similar result to the simulation result for the patch width (*w*) less than 18mm and greater than 30mm. Finally, the resonant frequency for the variation of dielectric substrate thickness is shown in Figure 10. It is found that the thicker substrate causes lower resonant frequency of a unit cell. From the figure, it shows that the proposed formulation produces quite similar result to the simulation result for dielectric substrate thickness less than 2.4mm and greater than 4mm compared to previous formulation reported in [10].

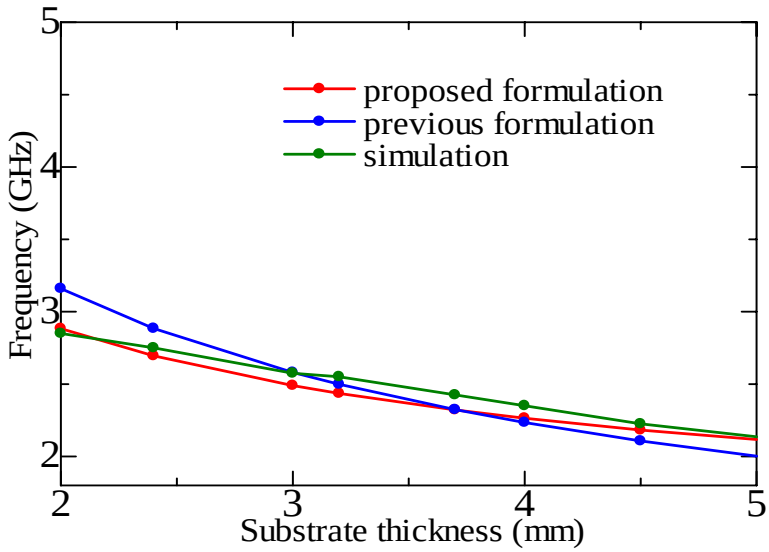

Figure 10. Comparison of resonant frequency for a unit cell with variation of dielectric substrate thickness (*t*)

4. Conclusions

The new formulation of resonant frequency for absorber based on AMC structure has been investigated theoretically based on analytical approach. The proposed formulation has been derived based on the dimension and property of a unit cell square patch of AMC structure. The simulation result of a unit cell of AMC structure has also been carried using commercialized software to be compared with the proposed formulation and the existing formulation provided by previous researcher. From the characterization results, it has been demonstrated that the resonant frequency of proposed formulation has similarity to the simulations on the patch width smaller than 17.5mm and bigger than 30mm with the thickness of dielectric substrate thinner than 2.4mm and thicker than 4 mm. Although there were some discrepancies between the proposed formulation result and the simulation result, however in general it could be concluded that the proposed formulations which has included all parameters in the calculation has shown better accurateness compared to the existing formulation. This will be a beneficial for the design of AMC-based devices such as absorber or reflectarray which requires high accuracy in result.

5. References

[1] C. Caloz and T. Itoh, Electromagnetic Metamaterials: Transmission Line Theory and Microwave Applications, *1st Edition, New Jersey: John Wiley & Sons Inc*., 2005

[2] N. Engheta and R. W. Ziolkowski, Electromagnetic Metamaterials: Physics and Engineering Explorations, *1st Edition, New Jersey: Wiley-IEEE Press*, 2006.

[3] R. Marqués, F. Martín and M. Sorolla, Metamaterials with Negative Parameters: Theory, Design and Microwave Applications, *1st Edition, New Jersey: John Wiley & Sons Inc*., 2008.

[4] D. Sievenpiper, L. Zhang, R Broas, N. G. Alexopolous, and E. Yablonovitch, "High-impedance electromagnetic surface with forbidden frequency band," *IEEE Trans. Microwave Theory Tech*., vol. 47, no.11, pp. 2059-2074, Nov. 1999.

[5] G. Goussetis, A.P. Feresidis, and J. C. Vardaxoglou, "Tailoring the AMC and EBG characteristics of periodic metallic arrays printed on grounded dielectric substrate," *IEEE Trans. Antennas Propagat.*, vol. 54, no. 1, pp. 82-89, Jan. 2006.

[6] A. Munir and V. Fusco, "Characterization of microwave anisotropic thin radar absorber using artificial magnetic groundplane," 2008 *Asia-Pacific Microwave Conference (APMC)* Proc., pp. 1-4, Hongkong, China, Dec. 2008.

[7] V. Fusco, A. Munir and M. Euler, "Planar two-bit phase encoded transpolarising reflector using textured surface technology," *3rd European Conference on Antennas and Propagation (EuCAP)* Proc., pp. 1386-1389, Berlin, Germany, Mar. 2009.

[8] Y. Zhang, J. Von Hagen, M. Younis, C. Fischer and W Wiesbeck, "Planar artificial magnetic conductors and patch antennas," *IEEE Trans. Antennas Propagat*., vol. 51, no. 10, pp. 2704-2712, Oct. 2003.

[9] A. Munir and V. Fusco, "Effect of surface resistor loading on high impedance surface radar absorber return loss and bandwidth," *Microwave and Optical Tech. Lett*., vol. 51, no. 7, pp. 1773-1775, Jul. 2009.

[10] D. Sievenpiper, High-Impedance Electromagnetic Surfaces, PhD Thesis, UCLA, 1999.

[11] S. Ramo, J. R. Whinnery and T. V. Duzer, Field and Waves in Communication Electronics, *3rd Edition, John Wiley & Sons*, 1994

[12] R. E. Collin, Foundation for Microwave Engineering, *2nd Edition, 'McGraw-Hill Inc*., 1992.

Levy Olivia Nur received the B.E. and M.E. degrees in Electrical Engineering, majoring in Telecommunication Engineering from Institut Teknologi Bandung, Indonesia, in 2001 and 2004, respectively. Currently, she is pursuing the doctorate degree at the same university. From 2002 to 2003, during her study in master program she joined the Japanese University Studies in Science & Technology (JUSST) at the University of Electro-Communications (UEC), Tokyo, Japan. From 2006 to 2010, she was a Lecturer at Indonesia Computer University (UNIKOM), Bandung, Indonesia. Since 2010, she has been joining the Telkom University (previously known as Institut Teknologi Telkom, ITTelkom) Bandung, Indonesia as Lecturer. Her research interest covers microwave absorbent material and its characterization.

Adit Kurniawan received the B.E. degree in Electrical Engineering from Institut Teknologi Bandung, Indonesia in 1986. He then received M.E. and Ph.D. degrees in Telecommunication Engineering from the RMIT University and the University of South Australia, in 1996 and 2003 respectively. Dr. Kurniawan is currently a Professor at the School of Electrical Engineering

and Informatics, Institut Teknologi Bandung, Indonesia. His research interest covers antenna and wave propagation, wireless cellular communications, and CDMA wireless communications.

Sugihartono received the B.E. degree in Electrical Engineering from Institut Teknologi Bandung, Indonesia in 1973. He received master and doctor degrees from the Ecole Nationale Superieure de l'Aeronautique et de l'Espace, Toulouse, France, in 1982 and 1987 respectively. Dr. Sugihartono is currently Associate Professor at the School of Electrical Engineering and Informatics, Institut Teknologi Bandung, Indonesia. His research interest covers digital communication system and communication signal processing.

Achmad Munir received the B.E. degree in Electrical Engineering from Institut Teknologi Bandung, Indonesia, in 1995, the M.E. and D.E. degrees in science and engineering from Yamaguchi University, Japan, in 2002 and 2005, respectively. From 2005 to 2007, he was a Research Fellow under JSPS fellowship program with department of Electrical and Electronics Engineering, Faculty of Engineering, Yamaguchi University, Japan, working on the artificial materials research, particularly, artificial dielectric and artificial magnetic materials. From 2007 to 2009, he was a Research Fellow with the Institute of Electronics, Communications, and Information Technology, Queens University Belfast, Northern Ireland, United Kingdom, involved in the experimental study of novel nonlinear artificial material including high impedance surface and artificial magnetic conductor for advanced EM applications. In January 2009, he joined the School of Electrical Engineering and Informatics, Institut Teknologi Bandung, Indonesia, as Lecturer. His research interests include linear and nonlinear artificial materials, electromagnetics wave propagation, and microwave devices.